

# We are IntechOpen, the world's leading publisher of Open Access books Built by scientists, for scientists

6,400

Open access books available

174,000

International authors and editors

190M

Downloads

Our authors are among the

154

Countries delivered to

TOP 1%

most cited scientists

12.2%

Contributors from top 500 universities



WEB OF SCIENCE™

Selection of our books indexed in the Book Citation Index  
in Web of Science™ Core Collection (BKCI)

Interested in publishing with us?  
Contact [book.department@intechopen.com](mailto:book.department@intechopen.com)

Numbers displayed above are based on latest data collected.  
For more information visit [www.intechopen.com](http://www.intechopen.com)



Chapter

# The Geomagnetic Field Transformants and Their Complexing with Data of Gravitational, Thermal and Radioactive Fields: During the Exploration of Hydrocarbon Fields at the Southern Part of the Ustyurt Region

*Abetov Auez Egemberdievich,*

*Yessirkepova Sharbanu Bakhytovna and Julia Barbosa Curto Ma*

## Abstract

The chapter discusses the results of the interpretation of aeromagnetic survey data in the southern part of the Ustyurt region in order to identify zones that are heterogeneous in magnetic properties, with their subsequent tie-up with areas promising for the detection of hydrocarbon accumulations. Three tectonic elements are distinguished—the Central Ustyurt system of disturbances, the Shakhpakhty step and the Assakeaudan depression according to the sign, orientation and quantitative values of the transformants of the geomagnetic field, and, consequently, according to the depth and extent of distribution of magnetized rocks, based on the degree of deformation of lithological-stratigraphic complexes and levels by deep faults. Within these tectonic elements, the transformants of the geomagnetic field were comprehensively interpreted with the data of gravitational, thermal and radiochemical fields to increase the reliability of the results of geological interpretation. This made it possible to study the behavior and characteristics of faults, to draw conclusions about the depth of gravitational and magnetically disturbing masses, about the degree of geological heterogeneity of large geosstructures, as well as to trace the nature of the manifestation of local structures in geophysical fields. The Central Ustyurt system of dislocation, the Shakhpakhty step and the Assakeaudan depression differ in varying degrees of active tectonics and differentiation by the degree of dislocation of oil and gas prospective objects, fragmentation by faults, by the extent of distribution of reservoir rocks and oil and gas source suite, conditions of conservation of hydrocarbon accumulations,

directions and channels of probable hydrocarbon migration, and assumptions are made about the relationship of oil and gas prospective structures and explored hydrocarbon field with large deep faults. The author's studies of transformants of magnetic and gravitational fields, geothermal and aerogamma spectrometry data clearly indicate in favor of the prospects of oil and gas potential of local structures of the Shakhpakhty step: Utezhai, Kozhantai, Northern Kozhantai, Otyynshy. In general, the results obtained will serve as a reliable basis for clarifying and detailing the geological and structural-formation models of the Southern Ustyurt, which can be used as the basis for the design of geological exploration for the exploration of new hydrocarbon field using expensive and time-consuming seismic exploration of CDP-3D and deep drilling.

**Keywords:** geomagnetic field transformants, airborne magnetic survey, magnetic anisotropy, high-frequency and low-frequency components, vertical and horizontal derivatives, Euler points, gravitational, thermal, and radiochemical fields

## **1. Introduction**

### **1.1 Geological setting**

The South Ustyurt region stands out on the southeastern margin of the South Mangyshlak sedimentary basin and is the eastern margin of the North Caucasian-Mangyshlak oil and gas province. This region is isolated as part of the South Mangyshlak oil and gas region, located within the Turan epihercynian platform.

In tectonic terms, the South Mangyshlak oil and gas region is located within a large area of Mesozoic intraplateform subsidence of the earth's crust, which is called the South Mangyshlak-Assakeaudan system of depression. This system is bounded in the north by the Mangyshlak-Central Ustyurt uplift zone, in the south by the northern periclinal of the Karabogaz arch and the Tuarkyr uplift zone, and in the west, it opens toward the Caspian Sea.

This system of depression has the shape of a triangle in plan, with the apex to the west and the base to the east. The axial part of this zone is complicated by a linearly elongated chain of bath-like depressions separated by structural saddles.

These depressions are distinguished by different areas and irregular, most often isometric shape in plan.

Along the axis of the South Mangyshlak-Assakeaudan system of depressions, the Zhazgurli, Uchkuduk, and Assakeaudan troughs are differentiated from west to east. Within each of these depressions, smaller depressions are of particular importance, complicating their structure.

A characteristic feature of the tectonics of the South Mangyshlak-Assakeaudan system depression is the stepwise subsidence of rocks from the boards of this system to its axial part. On the northern boards, the steps are located parallel or echelon to each other and generally subordinate the trend of the Mangyshlak-Central Ustyurt uplift zone.

Within the steps, chains of local uplifts of the anticlinal type are isolated, serving as traps for oil and gas. Local anticlinal folds are characterized by an asymmetric structure with a steep southern and more gently sloping northern wings and are slightly disturbed by faults.

The most ancient deposits, represented by thick strata of Upper Permian and Triassic rocks, are exposed in the areas of Mountain Mangyshlak. These rocks are drastically deformed and partially metamorphosed.

In the central and most submerged part of the South Mangyshlak oil and gas region, these occurrences are found at depths of more than 4 km. They are overlain by thick Jurassic sediments represented by all three sections, showing a drastic unconformity.

The stratigraphic completeness and thickness of these sediments within local tectonic elements are different. The Jurassic sediments in this area can reach a maximum thickness of 750 m. Traditionally, these sediments are associated with the main prospects for the exploration of hydrocarbon fields within the South Ustyurt. According to the conditions of sedimentation and the type of organic matter, the presence of main gas deposits is predicted here.

The rocks of the Jurassic complex with erosion and angular unconformity are overlain by deposits of the Cretaceous system, the eroded surface of which is overlain by Paleogene sediments.

Cretaceous deposits are widespread and are represented by the lower and upper sections.

**Lower Cretaceous:** The Neocomian complex includes sediments of the Barremian, Valanginian, and Hauterivian stages. At the bottom of the Neocomian stage, there is a layer of bluish-gray clay with a greenish tint from the Valanginian stage. This layer contains pyritized charred plant remains and thin interlayers of fine-grained sandstone. Above this layer, there is a sequence of interbedding sandstones, siltstones, and greenish-gray clays with the inclusion of Hauterivian fauna.

The Barremian is the thickest in the Neocomian. The lower part of the Barremian deposits is composed of red-colored clays with subordinate interlayers of siltstones and sandstones; the upper one is predominantly sandstone.

Below the red-colored sediments of the Barremian stage lies a layer of gray-colored rocks, which in the upper part transition to variegated Aptian rocks. The complex is composed of dark gray, silty, finely elutriated clays with charred plant remains.

The Albian stage is represented by dark gray clays with a greenish tint, thinly bedded, silty, with charred plant remains and pyrite. Sandstones are gray and greenish-gray, mostly weakly cemented, often turning into loose sands, quartz-feldspar, glauconite.

The Upper Cretaceous is represented by the Cenomanian, Turonian, Senonian, and Danish stages. The Lower Cretaceous sediments are lithologically subdivided into two complexes: terrigenous rock assemblages (Cenomanian, Turonian) and carbonate rock assemblages (Senonian, Danish).

In general, the above sediments are represented by terrigenous varieties, with the exception of the Upper Turonian-Danish carbonate deposits and layers of limestone-shell rocks in the sandy-clay section of the Neogene.

Paleogene deposits with erosion lie on the Cretaceous deposits and are represented by three sections. The thickness of the Paleogene sediments ranges from 0 to 632 m.

Paleocene sediments are represented in the lower part by greenish-gray clayey limestones, and in the upper part by brownish marls.

Eocene sediments consist of greenish-gray marls, and in the upper part of the section, they transition to dense, strong brownish-gray marls. These sediments contain remains of fauna, plant detritus, and pyrite.

The section of the Oligocene age is composed of clays of marine origin, which conformably lie on Eocene deposits. The clays in this section are greenish-gray with a bluish tint, and are interbedded with siltstone and sands. They are calcareous, and contain faunal remains as well as pyrite.

Neogene sediments are widespread and commonly overlie Oligocene rocks, characterized by erosion and angular unconformity. The Neogene section is divided into

two stages: the Tortonian and Sarmatian, which correspond in age to the Middle and Upper Miocene, respectively. Lithologically, the sediments are composed of marls and limestones, white, chalk-like, with inclusions of pyrite and gypsum. Sarmatian limestones make up the shell of the Ustyurt plateau. The thickness of the Neogene sediments ranges from 0 to 90 m.

The rocks of the Quaternary age lie on sediment deposits of different ages of the Cretaceous, Paleogene, and Neogene. The sediments are represented by brownish-yellow, quartz-feldspar sands and loose sandstones, siltstones, and gray loams. The thickness of the Quaternary deposits varies in the range of 0–15 m.

## **1.2 Data and materials**

The relevance of the application of effective innovative methods in the exploration of hydrocarbon fields is currently growing due to the emerging trend of depletion of oil and gas fields in operation.

An urgent task is to develop algorithms for solving geological problems to replenish Kazakhstan's mineral resource base through the exploration and development of new hydrocarbon fields [1, 2].

In 2019, LLP "SPC GEOKEN" Company performed integrated geophysical study to identify oil and gas prospective areas at the Central Ustyurt system of dislocation and in the southeastern part of the South Mangyshlak-Ustyurt system of depressions to solve these problems.

An independent role in these studies was assigned to aeromagnetic exploration with the solution of specific geological problems.

An aeromagnetic survey was conducted using the GT-MAG-2 airborne geophysical system, with flight lines spaced 1000 m apart and flown at an altitude of 100 m above the ground surface. The daily variations of the magnetic field were taken into account by the PBM Pico complex based on a CS-3 cesium magnetometer.

The TrimbleR7 GNSS L1/L2 dual-frequency GPS receiver was used as a ground reference station for geodetic referencing. The alignment accuracy of the survey route in plan was  $\pm 1$  m.

The field processing of aeromagnetic survey data was performed in two stages.

At the first stage, field processing was carried out, during which correction procedure was made for the deviation of instruments, daily variations in the magnetic field, and tie-up of survey lines using the statistical equalization method.

At the second, cameral stage, the following procedures were performed:

- a. calculation and input of corrections for radio-altimeter's readings and hypsometry of the day surface topography;
- b. filtering and correction of aeromagnetometry data;
- c. compiling of a base of magnetic variation data;
- d. calculation of normal and anomalous geomagnetic field and its most informative transformants;
- e. geomagnetic field transformants mapping and profiles plotting.

In order to extract the maximum geological information, the following transformants of the observed geomagnetic field were calculated [3]: analytical signal, vertical and horizontal gradients of the anomalous magnetic field, the angle of the magnetic field gradient vector, high-frequency and low-frequency components of the magnetic field, autotracing of the anomaly axes  $\Delta T_a$ , position of singular points Euler (**Table 1**).

Potential fields data	Transformants	Tectonic elements		
		Assakeaudan depression	Shakhpakhty fault terrace	Central Ustyurt uplift
Geomagnetic anomalies field	Anomalous magnetic field modified to the pole, nT.	From 100 to 300	From -50 to 100	From 100 to 400
	Analytic signal, nT/m.	From 0 to 0.007	From 0.005 to 0.01	From 0.003 to 0.03
	Tilt angle of TDR transformant, radian.	From 0 to 1.575	From -1.570 to 0	From -1.250 to 1.600
	Vertical derivative of geomagnetic field anomalies, nT/m	From -0.003 to 0.007	From 0 to -0.007	From -0.02 to 0.02
	Horizontal derivative of geomagnetic field anomalies, nT/m.	From 0 to 0.007	From 0 to 0.003	From 0.002 to 0.015
	Anisotropic transformant of the anomalous geomagnetic field, cu.	From 0 to 0.0025	From 0 to 0.0007	From 0 to 0.003
	Autotracing of axes of the anomalous geomagnetic field, cu.	From -0.7 to 1.5	From -3 to 0.7	From -3 to 6
Gravity anomalies field	Module of horizontal derivate of Bouguer anomaly, mG/m.	From 0 to 0.0015	From 0 to 0.0015	From 0 to 0.0033
	Module of the vertical derivate of Bouguer anomaly, mG/m.	From -0.002 to 0.001	From -0.001 to 0.001	From -0.003 to 0.004
	Local gravity anomaly (recalculated in the upper half-space at a height of 2.5 km), mG.	From -3 to 1	From -1.5 to 3	From -2 to 8
	Anisotropy transform, the accent of maximum gravity anomaly. Sliding window size 5 km × 2 km, cu.	From 0.1 to 0.46	From 0.1 to 0.48	From 0.1 to 0.50
Thermal anomalies field	Thermal field according to satellite imagery.	From 6162.9 to 6713.3	From 6106.4 to 6608.5	From 6237.7 to 6462.4
	Map of the regional component of the thermal field.	From 6297.8 to 6601.5	From 6283.1 to 6543.4	From 6319.8 to 6395
	Map of the local component of the thermal field.	From -182.2 to 152.8	From -211.2 to 64.8	From -65 to 69
	Map of the thermal field recalculated in the lower half-space. A cut at 1500 m.	From -17.2 to 16.6	From -17.9 to 12.6	From -10.5 to 12.6
	Map of the thermal field recalculated in the lower half-space. A cut at 2500 m.	From -20.8 to 20.9	From -22.2 to 12.1	From -8.9 to 9.8

Potential fields data	Transformants	Tectonic elements		
		Assakeaudan depression	Shakhpakhty fault terrace	Central Ustyurt uplift
Radiogeochemical anomalies field	Potassium value (K), %	From 0.5 to 1.3	From 0.4 to 1.3	From 0.6 to 1.3
	Thorium value (Th), ·10–4%	From 1.4 to 4.0	From 1.4 to 4.0	From 1.5 to 4.0
	Uranium value (U), ·10–4%	From 1.5 to 3.5	From 1.0 to 3.0	From 1.1 to 3.1
	Dose rate gamma radioactivity (DR)	From 16.6 to 38.2	From 13.9 to 36.5	From 16.7 to 37.2
	U/K, cu	From 1.7 to 4.1	From 1.6 to 3.7	From 1.7 to 3.5
	K/Th, cu	From 2.1 to 3.3	From 2.4 to 3.3	From 2.5 to 3.3
	U/Th, cu	From 0.6 to 2.0	From 0.7 to 2.3	From 0.7 to 2.0

**Table 1.**

*Statistics on the values of transforms of the anomalous magnetic and gravitational, thermal, and radiogeochemical fields.*

In the Geosoft Oasis Montaj software, matrices were built (with a cell size of 250 × 250 m) using the “Bidirectional Line Gridding” algorithm.

The international analytical model IGRF was adopted as the normal geomagnetic field of the Earth.

## 2. Results of the geological interpretation of the geomagnetic field transformants

### 2.1 Structure of the observed geomagnetic field

The poleward geomagnetic field in the study region is represented by linearly elongated  $\Delta T_a$  anomalies of both signs and is characterized by a northwest trend (**Figure 1A**).

The Karabaur swell is characterized by high values of the geomagnetic field intensity (+240 + 360 nT, in places up to +520 + 800 nT) with maximum values on the northern periphery of this swell, which indirectly indicates its dipping in the northern direction under the North Ustyurt massif.

The southern periphery of the Central Ustyurt system of dislocations is marked by a drastic decrease in the magnetization of rocks, which is demonstrated by the minimum values of the geomagnetic field intensity (up to  $\pm 50$  nT).

The boundary separating the Shakhpakhty step and the Central Ustyurt system of dislocations (Kolsai trough and Koskudyk swell) is distinguished by the minimum values of  $\Delta T_a$  anomalies (from +46 nT to +14 nT).

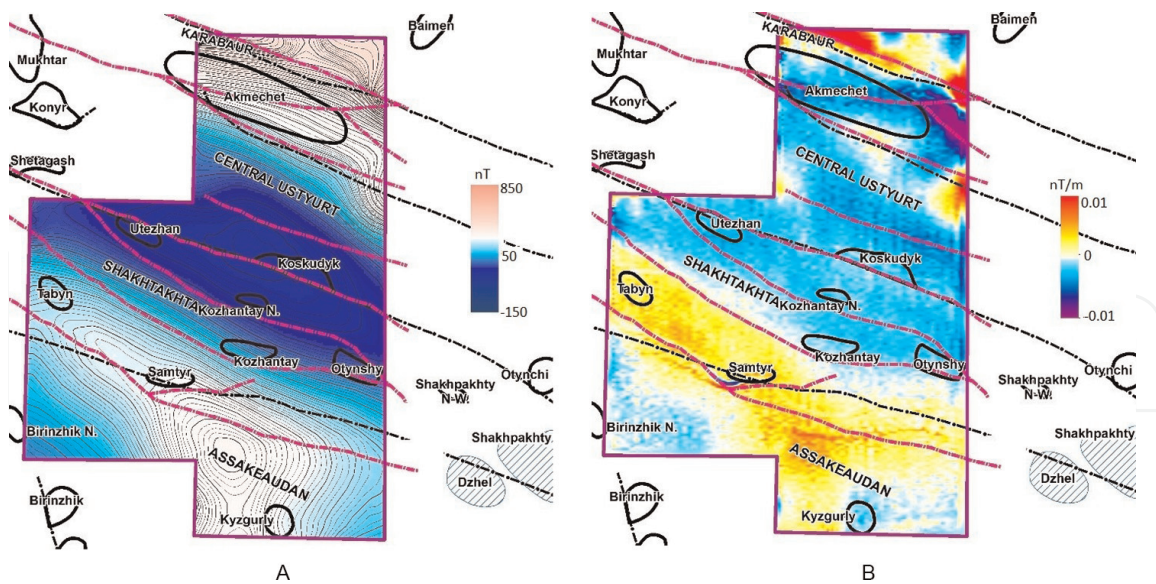


**Figure 1.** (A) Anomalous magnetic field reduced-to-the-pole; (B): Vertical derivative of the anomalous magnetic field reduced-to-the-pole. The dashed black lines indicate major faults along V reflecting horizon. Dashed pink lines indicate major tectonic break highlighted on a set of completed research (gravity exploration, magnetic prospecting, thermal fields, and ground surface).

The northern part of the Shakhpakhty tectonic step is characterized by a negative anomalous geomagnetic field (up to  $-50-100$  nT) on the local structures Utezhan, Koskudyk, Kozhantai, Northern Kozhantai, and Otyynshy (**Figure 1A**).

This circumstance indicates the formation of an anomalous geomagnetic field at the northern part of the Shakhpakhty step at a different time than at the Central Ustyurt fault system of dislocation and the Assakeaudan depression.

At the southern part of the Shakhpakhty step, another reversal of the geomagnetic field was revealed. Here, a high-gradient zone of positive anomalies  $\Delta T_a$  manifests itself with quantitative values up to  $+100 + 120$  nT (**Figure 1A**).

At the Assakeaudan depression, large anomalies of the geomagnetic field of northwestern orientation with an intensity of up to  $+300$  nT have been established (**Figure 1**).

## 2.2 Vertical gradient of the geomagnetic field

The tectonic boundaries between the Central Ustyurt system of dislocation, the northern and southern parts of the Shakhpakhty tectonic step, and the Assakeaudan trough show themselves sharply and rather contrastingly in the transformant ( $dZ$ ) of the geomagnetic field (**Figure 1B**).

The Assakeaudan depression is characterized by minimal variations in this transformant ( $-0.002 + 0.006$  nT/m), while the Shakhpakhty step exhibits intermediate values (0 to  $-0.006$  nT/m). The maximum values are observed at the Central Ustyurt system of dislocations ( $-0.01 + 0.01$  nT/m) (**Table 1**).

The vertical gradient of the geomagnetic field localizes anomalies, reveals the block structure of magnetic and non-magnetic rocks, emphasizes the high-frequency component, and makes it possible to see more clearly the structural and tectonic features along the chains of anomalies when mapping faults. Presumably, some of them were



migration of hydrocarbons in the presence of favorable structural and tectonic conditions.

If traps were encountered along the paths of migrating hydrocarbons, then the possibility of their filling is not excluded. In these cases, changes in the redox environment above the field are possible, leading to the formation of such ferromagnets as magnetite, hematite, pyrrhotite, which could be reflected in the structure of the high-frequency component of the geomagnetic field in the form of dissected and broken isodynamic lines.

Presumably, such processes occurred on the Utezhan, Kozhantai, Northern Kozhantai local structures, which is confirmed in the field of negative values of this transformant. However, this geological phenomenon needs further study.

### 2.3 Horizontal gradient of the geomagnetic field

The total horizontal poleward gradient was calculated by analyzing the lateral variability of the geomagnetic field (**Figure 2A**). The Shakhpakhty tectonic step exhibits intermediate values of the gradient of this transformant (from 0 to 0.002 nT/m), which increase to the north up to 0.010 nT/m, in the direction of the Central Ustyurt system of dislocations. Conversely, in the south direction, toward the Assakeaudan depression, the gradient decreases to 0 to 0.006 nT/m (**Table 1**). These findings directly confirm the presence of lateral inhomogeneities of magnetically disturbing masses in the study region.

### 2.4 Magnetic anisotropy

The magnetic anisotropy transformant, reduced to the pole (**Figure 2B**), shows the boundaries of anomaly-forming objects in contrast. To calculate this transformant, a sliding window size of 5 x 2 km was used.

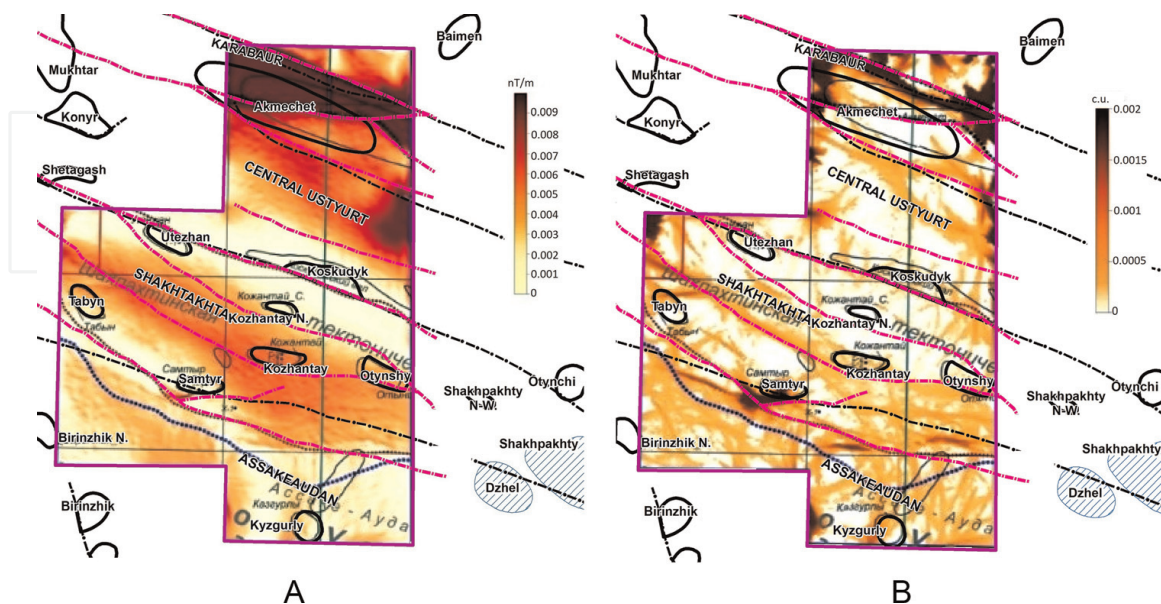


**Figure 2.**  
 (A) Module of the horizontal gradient of the geomagnetic field normalized to the pole. (B): Anisotropic transformant of the geomagnetic field normalized to the pole. Black dotted lines indicate major faults. Dashed pink lines indicate tectonic faults identified by the complex of studies performed (gravity exploration, magnetic prospecting, thermal fields, and day surface topography).

The southern and northern boundaries of the Shakhpakhty tectonic step, in the zone of its junction with the Assakeaudan depression and the Central Ustyurt system of dislocations (up to 0.002 standard units), are characterized by higher-than-usual values of the magnetic anisotropy transformant, which indicates an increase in the degree of heterogeneity of the basement rocks (**Table 1**).

Actually, the Shakhpakhty step is distinguished by reduced values of magnetic anisotropy (0–0.0005 standard units), including the Utezhan, Kozhantai, Northern Kozhantai, Otyynshy local structures (**Figure 2B**), which is considered as a favorable historical and geological factor that had an indirect sedimentary section.

## 2.5 Analytic signal

Several areas are distinguished according to the nature of the distribution of this transformant.

The areas of local structures Utezhan, Koskudyk, Kozhantai, Northern Kozhantai, and Otyynshy are characterized by lower values of the analytical signal, which are isolated in the northern part of the Shakhpakhty tectonic step and in the zone of its junction with the Central Ustyurt dislocation system.

To the southeast of these local structures within the Shakhpakhty tectonic step, but situated in the territory of the Republic of Uzbekistan, Shakhpakhty and Dzhel large gas fields were explored in the Upper Jurassic sediments.

To the south of the Shakhpakhty step, within the Assakeaudan trough, the transformant of the analytical signal exhibits the minimum values at the Kyzgurly, Birinzhik, and Northern Birinzhik local structures.

At the Central Ustyurt system of dislocations (Akmechet structure), increased values of this transformant are observed.

The revealed zonation is quantitatively confirmed by the values of the transformant of the analytical signal. At the Shakhpakhty step, they vary in the range of 0.005–0.008 nT/m, at the Assakeaudan depression they are 0–0.005 nT/m and at the Central Ustyurt system of dislocations they are 0.002–0.02 nT/m (**Table 1**).

A similar nature of the distribution of this transformant, apparently, is associated with: a) the general deepening of the upper edges of the magnetically disturbing masses in a southerly direction; and b) the block structure of the basement, in which magnetically active rocks of various scales are distributed.

## 2.6 The angle of the geomagnetic field gradient vector—TDR (tilt derivative)

This transformant (measured in radians) shows the maxima of the initial geomagnetic field regardless of their intensity and makes it possible to trace structural elements and map the position of the studied objects and their contours [4, 5].

The assessment of the depth of the studied objects is determined by the intensity of the TDR maxima (of both signs), which correspond to the axial lines of magnetically active objects. Zero values are their outer boundaries.

The northern part of the Shakhpakhty tectonic step is distinguished by the minimum values of TDR transformant (from –1.567 to 0 radians) normalized to the pole (Utezhan, Koskudyk, Kozhantai, Northern Kozhantai, and Otyynshy local structures) (**Table 1**).

Near values of this transformant (0–1.560 rad.) were recorded in the Assakeaudan depression and at the southern part of the Shakhpakhty step (Samtyr, Tabyn, Kyzgurly, Birinzhik, and Birinzhik northern structures).

The maximum negative values (−1.200–1.560 rad.) of the dip angles of the TDR transform (Akmechet structure) were found in the Central Ustyurt dislocation system.

### 2.7 Autotracing of axes of magnetic field anomalies normalized to the pole

This transformant is used to localize the axes of anomalies  $\Delta T_a$  (Figure 3) in order to identify faults, the presence of which is determined: a) by a sharp change in the intensity of the magnetic field along certain lines and b) by characteristic shifts of anomalous values relative to this line [6].

The axes of key anomalies help to distinguish the margin zone of Assakeaudan Depression, where the contact of which with Shakhpakhty Tectonic Step is revealed by a narrow boundary.

Minimal variations were observed in the auto-tracing of the axes of the geomagnetic field anomalies, which were normalized to the pole, in the Assakeaudan depression (−0.5 + 1 standard units). In contrast, intermediate values were found at the Shakhpakhty step (+0.5 to −3 standard units). The maximum values were established within the Central Ustyurt system of dislocations ( $\pm 5$  standard units), which is probably due to the involvement of this regional structure in the Late Paleozoic tectogenesis (Figure 3).

### 2.8 Depth distribution of special Euler's points

The depth distribution of magnetically disturbing masses is well illustrated by the Euler deconvolution solutions calculated in the Oasis Montaj software. We used a structural index of 1 with a window size of 20 km<sup>2</sup>.

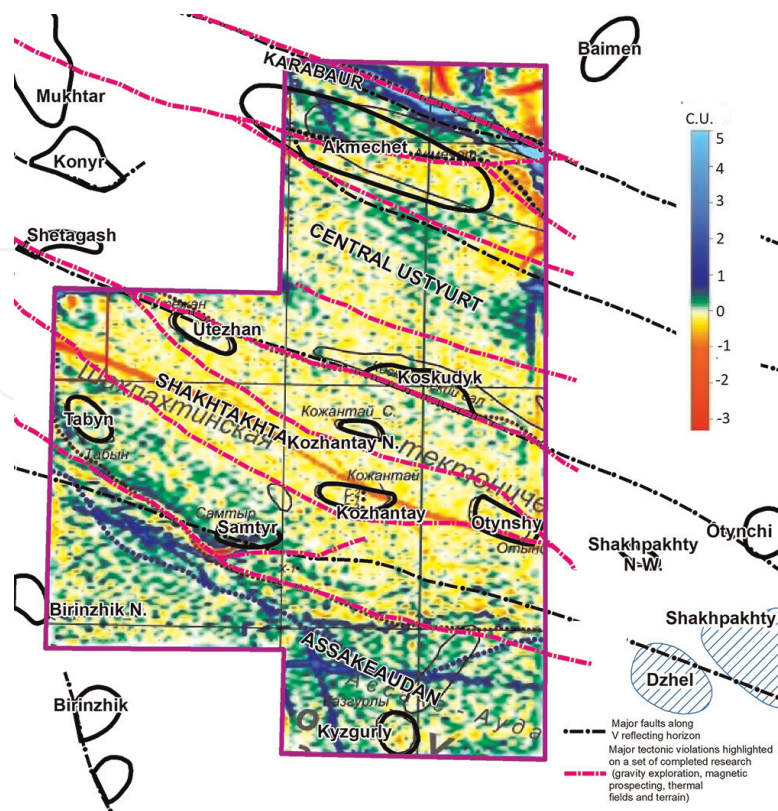


**Figure 3.**  
Tracing of axes of magnetic field anomaly, normalized to the pole.

Clusters of Euler points indicate an increased density of magnetic anomalies and their grouping into ordered lines can be used to trace the depths and contours of anomaly-forming objects or magnetically disturbing masses [7].

The schemes of the distribution of Euler points on depth and density (Figures 4–6) and the structure diagram of these points in geomagnetic fields (Figure 7) convincingly testify in favor of the inhomogeneous magnetization of rocks occurring at different depths, which is also indicated by the previously considered transformants of the geomagnetic fields.

The distribution of magnetically disturbing masses in the study area is sharply differentiated on area and depth. For example, in the depth interval of 6–11 km in the northern part of the Shakhpakhta tectonic step, the Euler points are grouped into NE-trending bands (Figure 5).

Their position is not controlled by the fault. From which we can conclude that the faults identified here do not have “deep roots.”

At the southern part of the Shakhpakhty tectonic step and at the Assakeaudan depression, Euler points form clouds of variable orientations from sublatitudinal to submeridional (in the depth interval 6–11 km), which call into doubt the tying between the genesis of magnetically disturbing masses and fault tectonics.

An indirectly revealed fact indicates a large total thickness of the rocks of the sedimentary cover and the quasi-platform cover on the Shakhpakhty tectonic step, which in turn indicates this tectonic element as favorable from the point of view of their oil and gas potential.

And finally, at the Central Ustyurt system of dislocations, the Euler points are grouped in the form of a zone of northwest orientation in the depth interval of

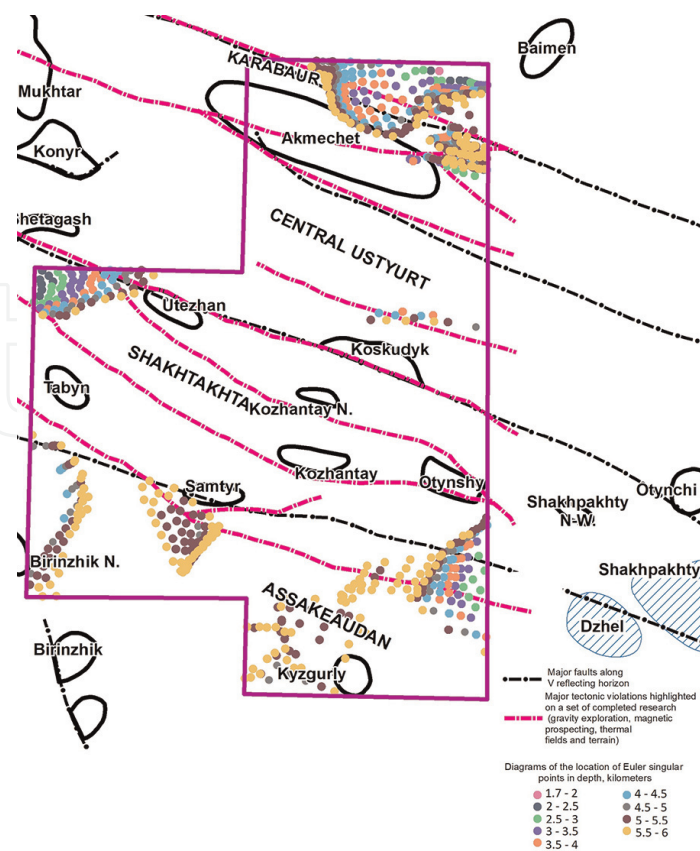


**Figure 4.**  
 Scheme of distribution by depth and density of Euler points (up to 6 km) of the geomagnetic field.

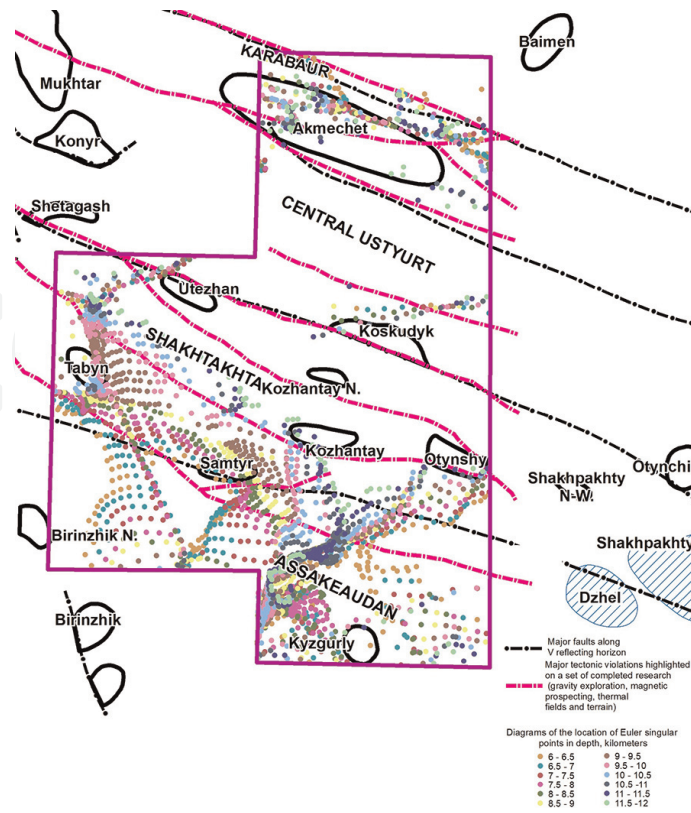


**Figure 5.**  
Scheme of distribution by depth and density of Euler points (in interval 6–11 km) of the geomagnetic field.

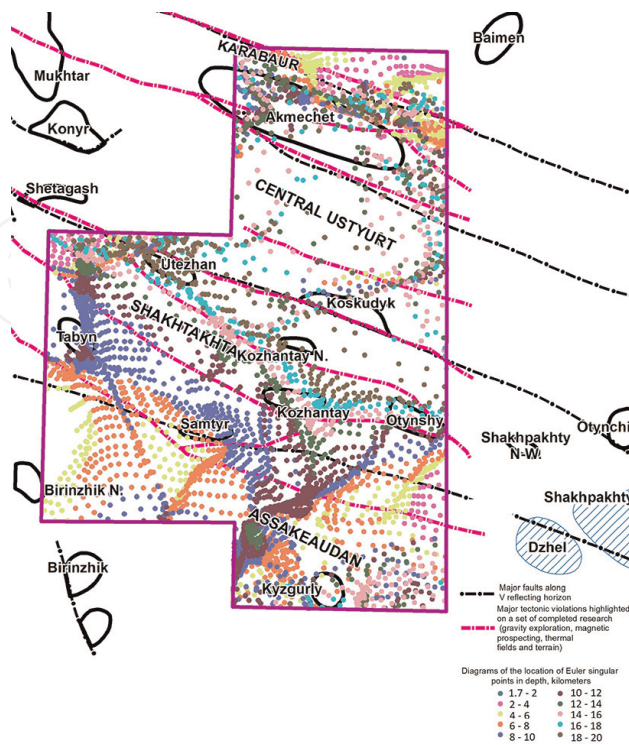


**Figure 6.**  
Scheme of distribution by depth and density of Euler points (up to 20 km) of the geomagnetic field.

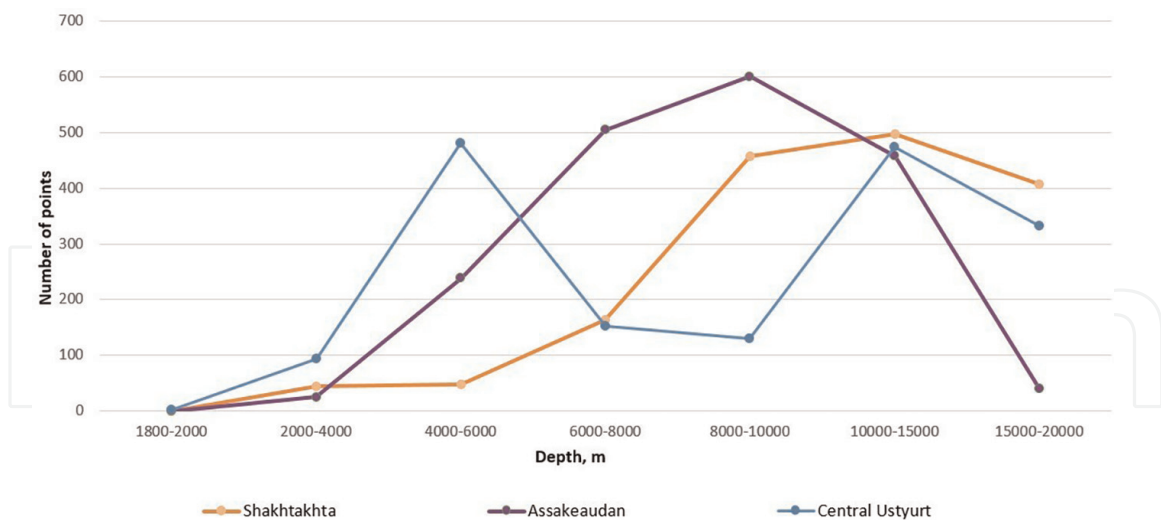


**Figure 7.**  
Graph of the distribution of Euler points by regions in geomagnetic models.

6–11 km (**Figure 5**). The orientation of the zone of increased density of Euler points is consistent with the direction of deep faults, which is the basis for talking about their paragenetic relationship.

Additionally, the Central Ustyurt system of dislocations revealed the presence of another depth interval (10–15 km) with the highest concentration of Eulerian singular points (**Figure 7**). This finding indirectly suggests that the Karabaur swell has subsided in a northern direction under the North Ustyurt massif, resulting in a “double” crustal effect. However, this assumption needs further serious verification with the construction of three-dimensional geological and geophysical models.

Another feature of the specific Euler points has been revealed in all three regional tectonic structures considered above. A sharp or “jump-like” increase in the density of these points in the depth interval of 6–11 km is observed (**Figure 5**).

Considering the distribution of Euler points at various depths in geomagnetic models, it is possible to preliminarily conclude that the top edge of magnetically disturbing masses within the Central Ustyurt system of dislocations occurs at intervals of 4–6 km and 10–15 km depths, while the Assakeaudan Depression sees such occurrences at a depth of 8–10 km, and the Shakhpakhty tectonic step sees it at a depth of 10–15 km.

Analyzing the distribution density of Euler points in the depth interval up to 6 km (**Figure 4**), it is important to note their minimum values throughout the study region, which form small fields with an implicit orientation. It can be assumed that intrusions of the basic composition into the quasi-platform cover took place here.

And finally, the depth interval is up to 20 km. In the Assakeaudan trough, in the Shakhpakhty step, and in the Central Ustrta system of dislocations, there are no differences in the distribution density and orientations of the Euler points, which in turn indicates the basement of these tectonic elements (**Figure 6**).

## 2.9 Distribution of Euler points based on gravimetry data

The geological informativeness of the models built on the basis of the data of magnetically disturbing masses would be insufficient without the involvement of data about the depths of occurrence of gravity-disturbing objects.

The special Euler points, calculated in the Geosoft Oasis Montaj software using the algorithm of three-dimensional deconvolution [8], are concentrated near the edges of the anomalies, and correspond to the position and depth of anomaly-forming or gravitationally-disturbing bodies [9].

The regional structural elements are reliably identified with the distribution of density inhomogeneities in depth based on the distribution of Euler points, as well as with the involvement of other transformants of the gravitational field. Theoretical calculations show that even if the Euler points do not form dense clusters near anomalous bodies, at least in their vicinity, the distribution density of these points becomes the highest.

The scheme (Figure 8) and the table (Table 2) of the location of Euler singular points in the depth range from 0.6 to 8.0 km, as well as the graph of the distribution of these points in the vertical geological section (Figure 9) convincingly testify in favor of the density differentiation of rocks according to their depth.

The geological orientation of gravity-disturbing objects at the South Ustyurt is drastically differentiated by area. For example, in the 2–8 km depth interval in the northern part of the Shakhpakhty step, Euler points are grouped into bands of north-eastern geological strike (Figure 9).

In the Central Ustyurt dislocation system, special Euler points are concentrated in swathes of predominantly northwestern geological orientation.

In the south of the Shakhpakhty tectonic step and in the Assakaudan depression, these points form a cloud extending in a submeridional direction.

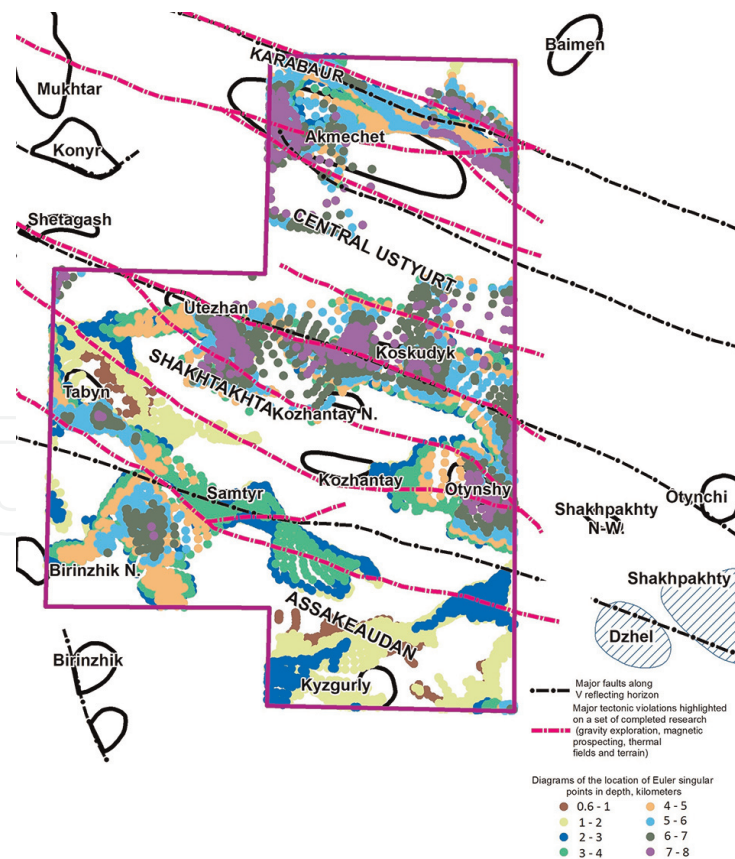


**Figure 8.**

Schematic diagram of the Euler points location in the gravitational field at depths up to 8.0 km (with an interval of 1.0 km). Legend: Black dotted lines represent faults complicating the structure of the V reflecting horizon. Dotted pink lines indicate deep faults identified by a set of geophysical data (gravity survey, magnetic survey, and thermal fields).

Regional structures	600–1000	Up to 2000 m	Up to 3000	Up to 4000	Up to 5000	Up to 6000	Up to 7000	Up to 8000
Central Ustyurt uplift	0	40	155	420	1765	810	255	240
Shakhpakhty fault terrace	0	42	245	460	500	585	610	280
Assakeaudan trough	190	1930	1390	1010	690	675	295	7

**Table 2.**  
 Locations of Euler points in the depth interval of 600–8000 meters.

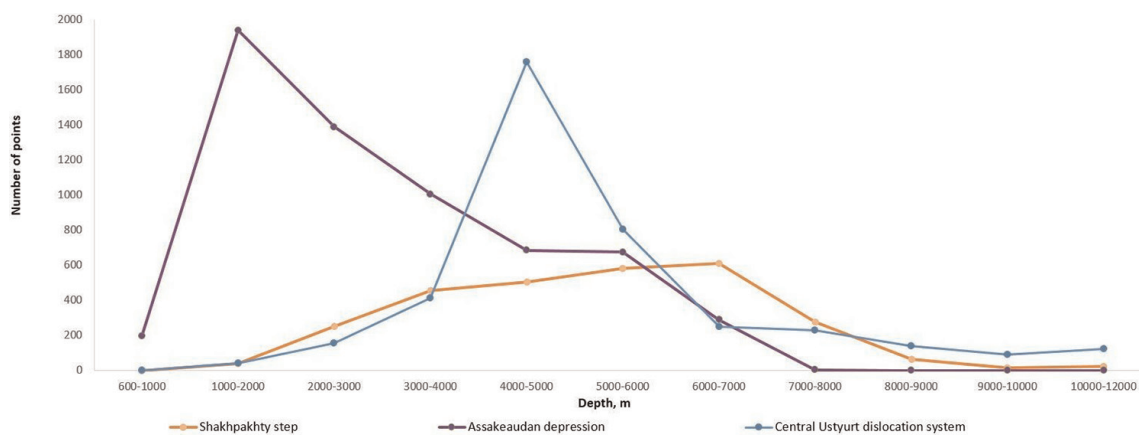


**Figure 9.**  
 Graph of the distribution of special Euler points based on gravimetry data (calculated in the Geosoft Oasis Montaj software).

At the Assakeaudan depression, the maximum number of Euler points on the surface of gravity-disturbing bodies is concentrated at depths up to 2000 m, in the Central Ustyurt dislocation system at depths up to 5000 m, and in the Shakhpakhty step at depths up to 6000 m (Table 2).

Figure 9 generally demonstrates a similar pattern, revealing significant variations in the depths of occurrence of gravity-disturbing bodies in all three regional structures, even at depths of 6000–7000 m. Deeper, these differences are significantly leveled. It can be assumed that this phenomenon is associated with a general transition from the formations of the quasi-platform cover to the rocks of the consolidated basement.

Considering the correlation of the depths of occurrence of gravitational and magnetically disturbing masses [10], it can be noted that accumulations of magnetically disturbing bodies in the Central Ustyurt dislocation system are observed in the depth intervals of 4000–6000 m. It is important to note that the depths of the occurrence of gravitationally and magnetically disturbing bodies coincide.

Based on CDP-2D seismic data, the depth of the basement surface at the Central Ustyurt dislocation system varies significantly, ranging from 4 to 8 km. The structures identified on this surface are linearly elongated, have a northwestern orientation, and are characterized by a general deepening in a southerly direction. In the area of the Akmechet local structure, the basement surface deepens to 9 km [11].



Consequently, the variations in the depths of the basement according to the CDP-2D seismic data are correlated in depth with the distribution of Euler points according to the gravity data.

It is important to note that in the Assakudan depression a serious discrepancy between the depths of occurrence of gravity-disturbing objects and magnetically disturbed masses was revealed.

The upper edge of the gravity-disturbing masses embeds at depths of 1000–2000 m and, apparently, reflects the transition from unconsolidated and weakly consolidated Lower Cretaceous rocks to more consolidated and epigenetically altered Upper Jurassic deposits. A similar phenomenon was revealed in some areas of the North Ustyurt region [7].

The upper edge of the magnetically disturbing masses here deepens to 8–10 km, which corresponds to the basement surface composed of rocks of basic and ultrabasic composition.

Interpretation data of the geomagnetic field anomalies are well correlated with the results of interpretation of the seismic CDP-2D data, which indicate that on the northern board of the Assakeaudan depression, the top of basement is deepened in a southerly direction from 7 to 10 km (at the Birinzhik local structure).

In contrast, a trend of uplift in the south-west direction can be observed along the top of the Upper Jurassic sediments (III reflecting horizon) from Kazgurly local structure, where it ranges from 2.6–2.8 km, to Birinzhik and Northern Birinzhik local structures, where it ranges from 1.7–2.0 km [11].

Therefore, we can talk about the correlation of the upper edge of the gravity-disturbing bodies with the top of Upper Jurassic sediments, while the upper edge of the magnetically disturbing masses is distinguished in the interval of depths of the top of basement.

*At the Shakhpakhty step*, a discrepancy was revealed in the position of the upper edges of the magnetic- and gravity-disturbing masses, which are submerged, respectively, to depths of 8–12 km and 6–7 km. The distribution pattern of these features suggests that there are differences in the depths of the basement and the quasi-platform cover.

This conclusion is confirmed by CDP-2D seismic data, based on which the depth of subsidence of the top of the Upper Paleozoic carbonate-terrigenous (quasi-platform cover) deposits varies in a wide range (from 3.8 km on the Tabynt structure, 4.5 km on the Samtyr and Utezhan structures, and up to more than 5.5 km on the Kozhantai and Otyynshi structures).

The structures at the top of the Upper Paleozoic carbonate-terrigenous sediments here have polygonal shapes and mosaic character, as well as a general deepening trend in the southeast direction. The exception is the local structure of Tabynt with a northwestern orientation and brachianticlinical forms.

It is difficult to speak about the depth of the top of basement according to CDP seismic data, since this boundary does not have good acoustic rigidity.

Consequently, at the Shakhpakhty step, the upper edges of the gravity- and magnetically disturbing masses are characterized by maximum depth. At the Assakeaudan depression, these physical inhomogeneities have a large spread in depth, while in the Central Ustyurt system of dislocations, they are distinguished by small fluctuations in the depth of occurrence.

Conclusions obtained as a result of integrated interpretation of magnetometry and gravimetry data are confirmed by airborne gamma ray spectrometer (radiometric) data processed and interpreted by the thorium normalized method [12, 13].

Thus, the Tabynt, Kozhantai, Northern Kozhantai, Utezhan, and Kyzgyrly local structures are recognized as potentially promising for the search and exploration of

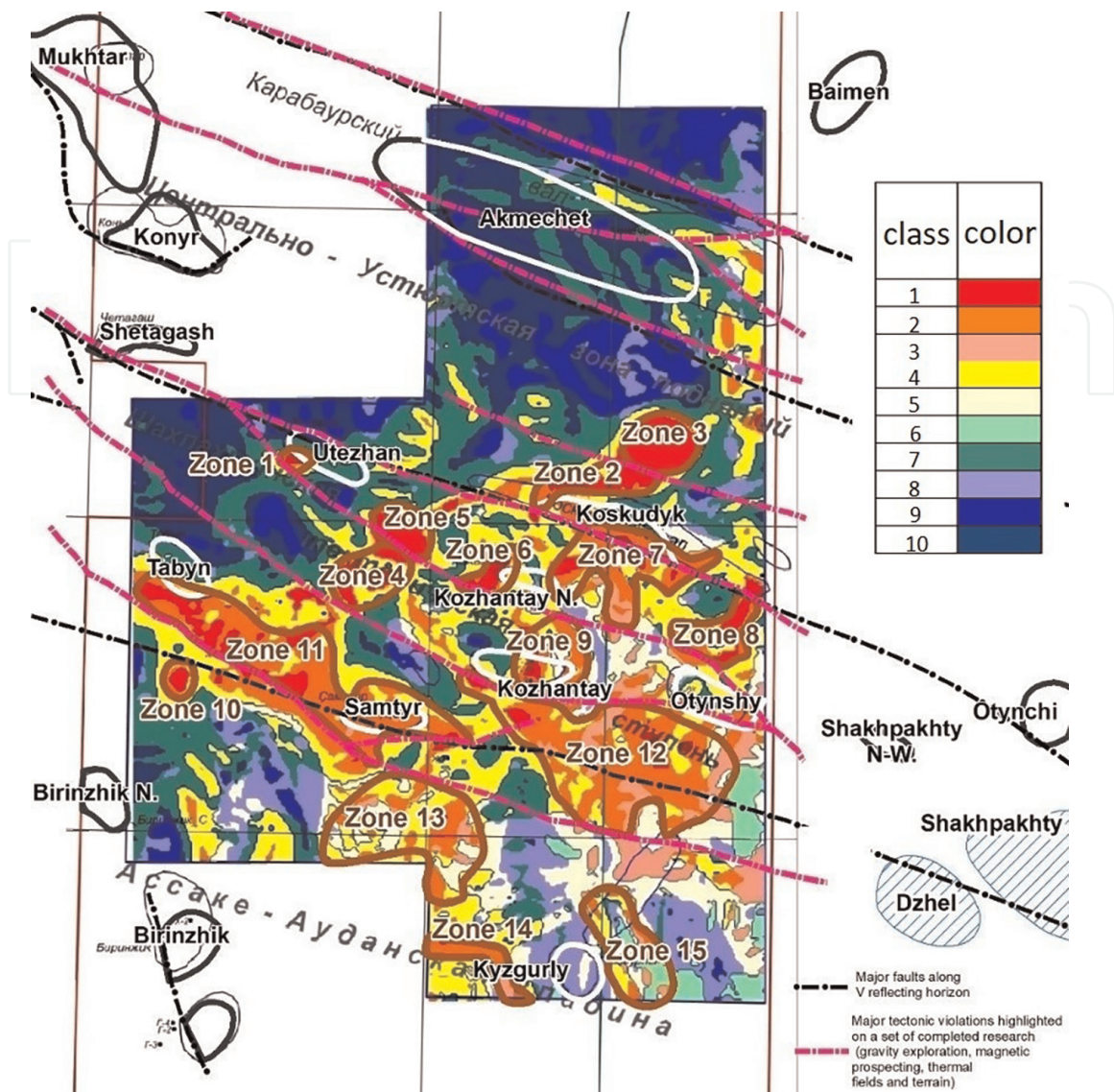


**Figure 10.** Zonation of the area according to the RAE (radioactive) parameters (according to the algorithm of A.V. Petrov).

hydrocarbon deposits based on the data of the interpretation of the anomalous magnetic field and the parameters of potassium and uranium content (**Figure 10**). And further, it is recommended to carry out detailed study of these structures using the seismic CDP-3D and deep drilling.

### 3. Discussion

All of the above allows us to draw the following conclusions: According to the nature of the distribution of geomagnetic field transformants (using data on gravitational, radioactive, and geothermal potential fields), the Shakhpakhty tectonic step, the Assakudan depression, and the Central Ustyurt system of dislocations are distinguished.

#### 3.1 Assakeaudan depression

It is identified by large positive anomalies in the northwest-orientated geomagnetic field, as well as high values in the transformants of magnetic anisotropy and the

derivative of the angle of inclination of the geomagnetic field vector. Conversely, the minimum values are observed in the transformants of the analytical signal, the vertical derivative, and the autotracing of the axes of the  $\Delta T_a$  anomaly (**Table 1**).

The author's materials on study of gravitational, thermal, and radiation fields were involved in order to increase the reliability and geological information content of the research results.

Within the Assakeaudan depression, minimum or reduced values of the modules of the horizontal and vertical gradients of the Bouguer gravity anomalies, local negative gravity anomalies (recalculated to the upper half-space at a height of 2.5 km) are distinguished based on the results of a quantitative interpretation of the gravity field [9].

The upper edge of the causative magnetic masses drops to a depth of 8–10 km, which corresponds to the depths of the basement rocks (according to seismic CDP-2D) and reflects the level of maximum propagation of basic and ultrabasic rocks into the basement [14].

The spatial location of special Euler points in the gravity field calculated in the Geosoft Oasis Moptaj software [8] indicates the presence of rock density heterogeneity up to a depth of 8.0 km. Deeper, the differences in the depths of the Euler points in terms of density inhomogeneities are significantly leveled.

The upper edge of gravity-disturbing masses at the Assakeaudan depression stands out at depths of 1000–2000 m and is confined to the III reflecting horizon (according to seismic CDP-2D) and reflects the transition of unconsolidated and weakly consolidated Lower Cretaceous rocks to Upper Jurassic sediments [11].

Within the Assakeaudan trough based on the interpretation of geothermal fields [15] to a depth of 5 km, a vast area of low geothermal anomalies with small local maxima in the upper part of the geological section to a depth of 2.0 km is distinguished.

The evidence in favor of the completion of this depression by rocks with low thermophysical properties and a relatively isotropic geological structure is supported by the following: minimal values of the Bouguer anomaly horizontal and vertical gradient module transformants, local negative gravity anomalies (recalculated in the upper half-space at a height of 2.5 km), autotrace of the axes of the  $\Delta T_a$  magnetic field anomalies, and reduced values of TDR transformant [4, 14].

At the Assakeaudan depression according to the airborne gamma spectrometry survey data identified 4 anomalous zones with a relatively reduced background of total radioactivity, low isoconcentrations of radioactive potassium isotope; reduced uranium content in relation to the background values (**Table 1**). The formation of these zones is associated with the effect of hydrocarbon microseepage [16, 17] along the regmatic faults network and macrofracture systems, which indirectly indicate the presence of gas or oil fields [12, 18].

### 3.2 Shakhpakhty tectonic step

It is distinguished by low values of the transformants of the analytical signal, autotracing of the anomaly axes  $\Delta T_a$ , magnetic anisotropy, minimal values of the TDR transformant, high values of the intensity of negative anomalies  $\Delta T_a$ . Here, increased values of the transformants of the horizontal and vertical derivatives of the geomagnetic field are observed [5].

In general, these characteristics testify to the continuity of tracing the rock assemblages along their strike.

At the same time, in contrast to the Assakeaudan depression, at the Shakhpakhty step, increased values of the vertical gradient of gravity anomalies

were revealed (**Table 1**), which indirectly may indicate an increased vertical variability of rocks.

Other characteristics of geophysical potential fields can be attributed to weakly and moderately intense local positive and negative Bouguer anomalies (recalculated to a height of 2.5 km) and increased values of intensity of negative anomalies, such as  $\Delta T_a$  (**Table 1**).

Within the Shakhpakhty step, the upper edge of the magnetically disturbing masses is submerged to depths of up to 8–12 km, while the gravity-disturbing bodies are deepened to 6.0–7.0 km. Apparently, the difference in their distribution demonstrates the difference in the occurrence depth of the tops of basement and the quasi-platform cover [11, 14].

Consequently, we can say that at the Shakhpakhty step, the upper edges of the gravity- and magnetically disturbing masses are distinguished by the maximum depth at the South Ustyurt region.

In turn, this fact is evidence in favor of the high total thickness of the sedimentary cover and the quasi-platform cover on the Shakhpakhty step, which unambiguously puts it in the category of prospective for hydrocarbon accumulation discoveries.

Shakhpakhty step is characterized by relatively large positive anomalies in the thermic fields, which indicates the predominance of rocks with high values of thermophysical properties (**Table 1**).

On the geological section that intersects the Shakhpakhty Step, where the gas field in the Uzbek part of Ustyurt has been explored, a relatively strong negative geothermic anomaly can be observed up to depths of 3000 m. This negative anomaly is further complicated in the upper part by two positive anomalies that reach maximum depths of 2200–2500 m.

However, it is known from literary sources [19, 20] that large gas field is marked by relatively negative thermal field anomalies, and positive anomalies in the upper part of the section, probably, are associated with compaction, providing a good “seal.” However, this interpretation of thermic anomalies requires additional study in the process of integrated analysis, including data of high-precision gravity survey, seismic survey, and drilling.

On this step, according to airborne gamma spectrometry survey on the ground surface, the maximum number of zones (9 out of 15 in the South and Central Ustyurt regions) with anomalously low of radioactive potassium isotope and uranium concentration in relation to the background values was detected, which may indicate increased prospects for oil and gas content in local structures [12].

### 3.3 Central Ustyurt system of dislocations

Within this large tectonic element, the maximum values of the intensity of positive anomalies  $\Delta T_a$ , the transformants of the vertical derivative, and TDR vector inclination angle of the magnetic field, autotracing of the axes of the anomalies of this field, as well as increased values of the transformants of the analytical signal, magnetic anisotropy, and the horizontal derivative of the anomalies  $\Delta T_a$  were recorded [14].

In the surveyed area, there is a uniform characteristic of increased values of local gravity anomalies (recalculated in the upper half-space at a height of 2.5 km). Here, intermediate values of the transformants of the modules of the horizontal and vertical gradients of the Bouguer gravity anomalies are observed (**Table 1**).

Generally, the values of the transformants of the geomagnetic and gravity fields [9] may indicate an increased lateral and vertical heterogeneity of the rocks assemblage forming the Central Ustyurt dislocation system.

The maximum number of Euler points on the surface of gravity-disturbing bodies is concentrated at depths of –4000-5000 m.

The Central Ustyurt dislocation system displays gravity- and magnetically disturbing masses that coincide in depth and are confined to the basement surface, as identified by seismic CDP-2D [11].

An airborne gamma spectrometric survey conducted in this geostructure identified two zones with a relatively low background of total radioactivity. These zones exhibited low isoconcentrations of radioactive potassium isotope and reduced uranium content when compared to the background [12].

Thus, based on the foregoing, it can be argued that the integration of the magnetic field transformants with the data of aero gamma spectrometry and gravimetry indicates favorable prospects for the oil and gas potential of the Shakhpakhty step.

An indirect factor that testifies in favor of this is the large depth of immersion of the magnetically active layer associated with the basement rocks [10].

There was taken an attempt to tie-up the depth and character of distribution of magnetically active layers with areas potentially prospective for HC (hydrocarbon) accumulations to be detected.

In fact, the scientific novelty and practical significance of the obtained research results are the use of magnetic survey data for prospecting and exploration of hydrocarbon fields at the South Ustyurt.

Thus, the transformants of the initial geomagnetic field presumably increase reliability in detection of anomalous objects, and may be considered as an extra exploration criterion in prospecting and exploration of HC fields.

#### **4. Recommendations for exploration**

The focus of attention in the regional study should be placed on conducting exploration on local structures at the Shakhpakhty step, within which there is a deep plunge of the basement, the presence of thick strata of sedimentary cover and quasi-platform cover, and the increased positive anomalies of the thermal field were identified [21].

The integrated interpretation of data on the thermic field and the transformants of the gravity and magnetic fields, as well as aero gamma spectrometry (processed and interpreted by the thorium normalization method), suggest promising oil and gas prospects in local structures such as Utezhan, Kozhantai, Northern Kozhantai, and Otyynshi. This is attributed to favorable historical-geological, structural, and lithofacies factors (**Table 3**).

The location of these local structures is given in the figures above in the text.

The CDP-3D seismic survey and deep exploratory drilling with obligatory penetration of sediments of the quasi-platform cover are recommended on these local structures in order to explore new hydrocarbons accumulations.

#### **5. Conclusion**

The depth and nature of the spread of the magnetoactive layer in areas prospective for the detection of HC accumulations were successfully related using various the

Potential fields	Transforms	Structures of Jurassic-Cretaceous deposits revealed by CDP-2D seismic survey			
		Utezhn	Kozhantai N.	Kozhantai	Otyynshi
Geomagnetic anomaly field	Anomalous magnetic field reduced-to-the-pole, nT.	From -5.50 to 2.21	From -5.04 to 1.93	From 21.41 to 53.67	From 8.18 to 31.04
	Analytic signal, nT/m.	From 0.006 to 0.008	From 0.005 to 0.008	From 0.005 to 0.008	From 0.005 to 0.012
	Tilt derivative (TDR) of the magnetic field anomalies, radian.	From -1.56 to -1.23	From -1.36 to -0.94	From -0.80 to -0.05	From -1.36 to -0.24
	Vertical derivative of the anomalous magnetic field, nT/m.	From -0.004 to -0.001	From -0.003 to -0.001	From -0.003 to 0.00001	From -0.004 to 0.001
	Horizontal derivative of the modulus magnetic field, nT/m.	From 0.000 to 0.002	From 0.001 to 0.003	From 0.005 to 0.006	From 0.003 to 0.005
	Transformation of the magnetic field anisotropy, cu.	From 0 to 0.0003	From 0 to 0.0001	From 0.0005 to 0.001	From 0 to 0.0005
	Tracing of axes of magnetic field anomaly, cu.	From -0.57 to 0.53	From -0.68 to 0.26	From -1.92 to 0.39	From -1.77 to 0.34
Gravity anomaly field	Module of horizontal derivate of Bouguer anomaly, mGl/m.	From 0.0002 to 0.0010	From 0.0003 to 0.0008	From 0.00003 to 0.0007	From 0.0004 to 0.0010
	Module of the vertical derivate of Bouguer anomaly, mGl/m.	From -0.0004 to 0.0005	From -0.0007 to 0.0001	From -0.0006 to 0.0004	From -0.0004 to 0.0008
	Local gravity anomaly (recalculated in the upper half-space at a height of 2.5 km), mGl.	From -0.84 to -0.23	From -1.19 to -0.83	From -1.15 to -0.70	From -1.03 to -0.02
	Anisotropy transform, the accent of maximum gravity anomaly. Sliding window size 5 km x 2 km, cu.	From 0.1 to 0.12	From 0.1 to 0.11	From 0.1 to 0.14	From 0.1 to 0.14
Thermal anomaly field	Thermal field according to satellite imagery.	From 6266.32 to 6428.80	From 6281.45 to 6404.68	From 6333.09 to 6509.25	From 6442.89 to 6556.22
	Map of the regional component of the thermal field.	From 6311.40 to 6357.90	From 6369.59 to 6399.50	From 6380.17 to 6449.76	From 6495.36 to 6524.38
	Map of the local component of the thermal field.	From -26.54 to 50.10	From -76.65 to -17.70	From -38.34 to 51.75	From -49.79 to 29.48

Potential fields	Transforms	Structures of Jurassic-Cretaceous deposits revealed by CDP-2D seismic survey			
		Utezhan	Kozhantai N.	Kozhantai	Otyynshi
	Map of the thermal field recalculated in the lower half-space. A cut at 1500 m.	From -3.1 to 10.6	From -5.3 to 2.3	From -3.6 to 4.2	From -7.3 to 3.6
	Map of the thermal field recalculated in the lower half-space. A cut at 2500 m.	From -0.4 to 10.4	From -7.3 to -0.6	From -4.4 to 4.5	From -7.6 to 3.8
Radiogeochemical anomalies field	Potassium value (K), %	From 0.57 to 1.05	From 0.71 to 1.04	From 0.68 to 1.07	From 0.70 to 1.12
	Thorium value (Th), ·10 <sup>-4</sup> %	From 1.54 to 3.30	From 1.94 to 3.14	From 1.92 to 3.29	From 1.89 to 3.45
	Uranium value (U), ·10 <sup>-4</sup> %	From 1.70 to 2.56	From 1.64 to 2.46	From 1.61 to 2.47	From 1.90 to 2.51
	Dose rate gamma radioactivity (DR)	From 19.27 to 31.88	From 22.90 to 31.64	From 21.30 to 32.15	From 21.89 to 32.91
	U/K, cu	From 1.90 to 3.15	From 2.01 to 2.83	From 2.02 to 3.04	From 1.99 to 3.11
	K/Th, cu	From 2.66 to 3.18	From 2.70 to 3.12	From 2.68 to 3.09	From 2.58 to 3.13
	U/Th, cu	From 0.88 to 1.78	From 1.04 to 1.63	From 0.93 to 1.62	From 0.88 to 1.67

Note: TF—thermic field; MF—magnetic field.

**Table 3.** Statistics on transform values for anomalous magnetic, gravity, thermal, and radiogeochemical field transforms by local structures over the study region.

transformants of this field, such as analytical signal magnetic anisotropy, autotracing axes of magnetic field anomalies, increased values of negative anomaly  $\Delta T_a$ , and horizontal and vertical magnetic field gradients, as well as the minimum values of the TDR.

The results of an integrated analysis of the geomagnetic, gravitational, thermal, and radiochemical fields allowed the authors of this chapter to study the behavior and characteristics of tectonic faults, and to make some judgments about the depth of occurrence of gravity and magnetically disturbing masses, about the degree of geological heterogeneity of large geostructures, and to trace the nature of the manifestation of local structures in geophysical fields.

The Shakhpakhty step with a relatively increased thermal field in some local structures is quite clearly distinguished into the regional gravity, geomagnetic, and thermal fields, and has a continuation in the Uzbek part of this step.

The Shakhpakhty step is bounded by deep faults, identified by the gradients of anomalies of the regional geophysical fields. Three major regional faults are traced in the northwestern direction. On the southeastern flank of these faults, the Shakhpakhty and Dzhel gas fields are explored within the Jurassic sediments. On the western flank, the local structures Otyynshi, Kozhantai, Northern Kozhantai, Utezhan, and others close to them in geological structure are isolated.

These local structures can be considered as prospective in terms of the localization of HC accumulations, if there is a good seal of rocks in the upper part of the predicted reservoirs. All of the aforementioned criteria give reason to recommend local structures within the Shakhpakhty step for priority study.

Central Ustyurt system of dislocations is characterized by elevated deformation of sedimentary rock assemblage that does not contribute to the preservation of hydrocarbon accumulations.

The Assakeaudan depression is characterized by thick sedimentary rock assemblages, which generated mostly by the oil-source suites. Faults that disrupt the integrity of the geological formations of this depression are considered as conduits for migration of hydrocarbons, deep fluids, heat, and mass transfer.

This statement is confirmed by aero gamma spectrometry data, processed and interpreted by the method of thorium normalization. A total of 15 anomalous zones were identified in the study region, 9 of which are located in the Shakhpakhty step, 2 in the Central Ustyurt system of dislocations, and 4 in the Assakeaudan depression.

The selected anomalous zones have low values of isoconcentrations of radioactive potassium isotope and reduced uranium concentration in relation to the background values and are considered as indicative criteria for the possible presence of hydrocarbon accumulations.

Thus, our studies of the transformants of the magnetic, gravitational, and geothermal fields, airborne gamma spectrometry data (processed and interpreted using the thorium normalization method) unequivocally testify in favor of the prospects for the oil and gas potential of the local structures Utezhan, Kozhantai, Northern Kozhantai, Otyynshy, taking into account favorable historical and geological, structural, and lithofacies factors.

The author's study on advanced (relatively cheap) geophysical methods will provide a dependable foundation for enhancing and specifying the geological and structural-tectonic models of South Ustyurt. This will involve using existing information on the spatial distribution of already known oil and gas fields as well as serving as a basis for designing geological exploration to prospect and explore new hydrocarbon accumulations, using expensive and "heavy" methods of seismic exploration CDP-3D and deep drilling.



IntechOpen

### Author details

Abetov Auez Egemberdievich<sup>1\*</sup>,  
Yessirkepova Sharbanu Bakhytovna<sup>1</sup> and Julia Barbosa Curto Ma<sup>2</sup>


1 Kazakh National Research Technical University named after K. I. Satpayeva,  
Almaty, Kazakhstan

2 University of Brasilia, Brasilia, Brazil

\*Address all correspondence to: abetov.auez@mail.ru

### IntechOpen

---

© 2023 The Author(s). Licensee IntechOpen. This chapter is distributed under the terms of the Creative Commons Attribution License (<http://creativecommons.org/licenses/by/3.0>), which permits unrestricted use, distribution, and reproduction in any medium, provided the original work is properly cited. 

## References

- [1] Daukeyev SZ. Deep structure and mineral resources of Kazakhstan. In: Volume III Oil and Gas. Almaty; 2002. p. 248
- [2] Ozdoev SM. Prospects of oil and gas content in sedimentary basins of Kazakhstan. NEWS OF NAS RK, Series of geology and technical sciences. 2012;1:61-76
- [3] Blakely RJ. Potential Theory in Gravity and Magnetic Applications. Cambridge: Cambridge Univ. Press; 1996. DOI: 10.1017/CBO9780511549816
- [4] Castro FR, Oliveira SP, de Souza J, Ferreira FJF. Combining tilt derivative filters: New approaches to enhance magnetic anomalies. Brazilian Journal of Geophysics. 2018;37. DOI: 10.22564/rbgf.v36i3.1956
- [5] Saada SA. Edge detection and depth estimation of Galala El Bahariya plateau, Eastern Desert-Egypt, from aeromagnetic data. Geomech. Geophys. Geo-energ. Geo-resour. 2015;2:25-41. DOI: 10.1007/s40948-015-0019-6
- [6] Petrov AV, Nikitin AA. Coscad 3Dt. Complex of Spectral-Correlation Analysis of Geophysical Evidence, user's Manual Part I. Moscow: Russian State Geology Prospecting University; 2003
- [7] Abetov A, Niyazova A, Saurikov Z. 3D modeling of Euler's points for Geodensity and geomagnetic models of north Ustyurt region in Geosoft Oasis Montaj software. NEWS OF NAS RK, Series of geology and technical sciences. 2017;6:171-177
- [8] Montaj MAGMAP Filtering 2D Frequency Domain Processing of Potential Field Data Extension for Oasis Montaj. Vol. 7.12013
- [9] Matusevich AV. Structure of the local gravity field as a basis for zoning salt domes Caspian depression. News of NAS RK. Series of geology and technology sciences. 2006;5:65-76
- [10] Serkerov SA. Gravity and Magnetic Prospecting in Oil and Gas. Moscow: Oil and Gas. Gubkin Russian State University of Oil and Gas; 2006. pp. 501-512
- [11] Abetov AE, Yessirkepova Sh B, Curto MJ. Gravity Field Transforms at the Exploration for Hydrocarbon Field in the Southern Part of the Ustyurt Region. Vol. 3. NEWS OF NAS RK, Series of geology and technical sciences; 2022. pp. 17-31
- [12] Abetov AY, Essirkepova SB, Kozhamsugirov D. Effectiveness of aerogamma-spectrometric research in solving applied problems of oil and gas geology. Geologiya i okhrana nedr. 2021, 2021;78(1):55-62
- [13] Saunders DF, Burson KR, Branch JF, Thompson CK. Relation of Thorium-Normalized Surface and Aerial Radiometric Data to Subsurface Petroleum Accumulations. Vol. 58, N. 10. Tulsa, OK, United States: Society of Exploration Geophysicists; 1993. pp. 1417-1427
- [14] Abetov AE, Yessirkepova Sh B, Curto MJ. Geomagnetic Field Transforms and their Interpretation at Exploration for Hydrocarbon Field in the Southern Part of the Ustyurt Region. Vol. 6. NEWS OF NAS RK, Series of geology and technical sciences; 2021. pp. 6-14
- [15] Kronberg P. Remote study of the earth. In: Fundamentals and Methods of Distance Research in Geology. Moscow: World. Trans.; 1988. p. 343

[16] Saunders DF, Burson K, Thompson CK. Model for hydrocarbon microseepage and related near-surface alterations. *AAPG Bulletin*. 1999;**83**(1): 170-185

[17] Curto JB. The Role of Aero Geophysics for Detecting Hydrocarbon Microseepages and Related Structural Features: The Case of Remanso Do Fogo. Vol. 77, N. 2. Brazil: Geophysics; 2012. pp. B35-B41

[18] Klusman RW. Soil Gas and Related Methods for Natural Resource Exploration. New York: John Wiley; 1993. 483 p

[19] Shilin BV. Thermal Surveying in the Study of Natural Resources. Moscow: Gidrometeoizdat; 1980

[20] Gornyi VI, Shilin BV, Yasinskii GI. Thermal Aerospace Survey. Moscow: Nedra; 1993 128 p

[21] Abetov AE, Yessirkepova Sh B, Curto MJ. Remote sensing at the study of the thermal field of the South Ustyurt Region to find hydrocarbon deposits. *NEWS OF NAS RK, Series of Geology and Technical Sciences*. 2023;**2**:6-16